

# High-density QCD and Cosmic Ray Air Showers

H. J. Drescher<sup>a</sup>, A. Dumitru<sup>a</sup>, M. Strikman<sup>b</sup>

<sup>a</sup> *Johann Wolfgang Goethe University, Postfach 11 19 32, 60054 Frankfurt, Germany*

<sup>b</sup> *Department of Physics, Pennsylvania State University, University Park, PA 16802, USA*

We discuss particle production in the high-energy, small- $x$  limit of QCD where the gluon density of hadrons is expected to become nonperturbatively large. Strong modifications of the phase-space distribution of produced particles as compared to leading-twist models are predicted which reflect in the properties of cosmic ray induced air showers in the atmosphere. Assuming hadronic primaries, our results suggest a light composition near GZK cutoff energies. We also show that cosmic ray data discriminate among various QCD evolution scenarios for the rate of increase of the gluon density at small  $x$ , such as fixed-coupling and running-coupling BFKL evolution. There are clear indications for a slower growth of the gluon density as compared to RHIC and HERA, due e.g. to running-coupling effects.

PACS numbers: 13.85.-t, 13.85.Tp, 96.40.Pq

Today, the cosmic ray energy spectrum has been measured up to energies near the GZK cutoff,  $E \approx 10^{11}$  GeV [1, 2]. These energies by far exceed those reached by terrestrial accelerators. Thus, air showers induced in our atmosphere present a unique opportunity to probe high-energy QCD at very small light-cone momentum fractions  $x$ , i.e. in the regime of nonperturbatively large gluon densities. The physics of gluon saturation is therefore expected to play a significant role for the properties of extensive air showers, and thus for the determination of the nature of the highest energy cosmic rays. We refer to refs. [3, 4] for discussions regarding the relevance of high energy QCD interactions for air showers and composition analysis.

The high-energy limit of hadron scattering from a nucleus can be addressed from two complementary views. In the frame where the nucleus is at rest the partons up to the “black-body” resolution scale  $p_t(s)$  interact with the target with (nearly) the geometric cross section of  $2\pi R_A^2$ . Hence, in this limit the projectile wave function is resolved at a virtuality of  $\sim p_t^2$  which is much larger than any soft scale such as  $\Lambda_{\text{QCD}}$ . In this frame, the process of leading hadron production corresponds to releasing the resolved partons from the projectile wave function. The partons then fragment with large transverse momenta  $\sim p_t$  and essentially independently since their coherence was completely lost in the propagation through the black body. In the case of  $\gamma^*A$  scattering one is able to make nearly model independent predictions for the leading hadron spectrum [5] which differ drastically from the DGLAP leading-twist limit.

On the other hand, one could discuss the high density limit in the infinite momentum frame. Indeed, the wave function of a fast hadron (or nucleus) exhibits a large number of gluons at small  $x$ . The density of gluons is expected to saturate when it becomes of order  $1/\alpha_s$  [6]. The density of gluons per unit of transverse area at saturation is denoted by  $Q_s^2$ , the so-called saturation momentum. This provides an intrinsic momentum scale [7] which grows with atomic number (for nuclei) and with rapidity, due to continued gluon radiation as phase space grows. For sufficiently high energies and/or large nuclei,  $Q_s$  can become much larger than  $\Lambda_{\text{QCD}}$  and so weak coupling methods are applicable. Nevertheless, the well-known leading-twist pQCD can not be used precisely because of the fact that the density of gluons is large; rather, scattering amplitudes have to be resummed to all orders in the density. When probed at a scale below  $Q_s$ , cross sections approach their geometrical limit over a large range of impact parameters, while far above  $Q_s$  one deals with the dilute regime where they can be approximated by the known leading-twist pQCD expressions.

The target nucleus, when seen from the projectile fragmentation region, is characterized by a large saturation momentum. Its precise value can not be computed from first principles at present but model studies of deep inelastic scattering (DIS) at HERA suggest

$$Q_s^2(x) \simeq Q_0^2 (x_0/x)^\lambda \quad (1)$$

with  $x_0$  a reference point and an intercept  $\lambda \approx 0.3$  [8]. The initial condition at  $x_0$  accounts for the growth of  $Q_s$  with the number of valence quarks; for example, near the rest frame of the nucleus one might fix  $Q_0^2 \propto A^{1/3} \log A$ , with a proportionality constant of order  $\Lambda_{\text{QCD}}$  [7]. [We remark that for realistic nuclei  $Q_s$  does of course also depend on the impact parameter, which we don't spell out explicitly.]

The above scaling relation can be obtained from the *fixed coupling* BFKL evolution equation for the scattering amplitude of a small dipole. The BFKL equation is a linear QCD evolution equation which can not be applied in the high-density regime. Nevertheless, one can evolve the wave function of the target in rapidity  $y = \log 1/x$  and ask when the dipole scattering amplitude becomes of order one, which leads to  $Q_s^2(y) = Q_s^2(y_0) \exp c\bar{\alpha}_s y$  [9], with  $\bar{\alpha}_s = \alpha_s N_c / \pi$  and  $c \approx 4.84$  a constant. Hence, LO fixed-coupling BFKL evolution predicts  $\lambda' = c\bar{\alpha}_s$  of order one, a few times larger than the fit (1) to HERA phenomenology. A NLO BFKL analysis corrects this discrepancy and leads

to  $\lambda'$  much closer to the phenomenological value [10]. A similar observation is made in [11] where both  $\log(1/x)$  and  $\log Q$  effects were considered. The approach from the leading-twist regime to the black-body limit (BBL) has also been studied using the DGLAP evolution equation in ref. [12].

On the other hand one could also consider BFKL evolution with ad-hoc one-loop running of the coupling [9, 13]:  $\bar{\alpha}_s(Q_s^2) = b_0/\log(Q_s^2(x)/\Lambda_{\text{QCD}}^2)$ , which leads to

$$Q_s^2(y) = \Lambda_{\text{QCD}}^2 \exp \sqrt{2b_0 c(y + y_0)}, \quad (2)$$

with  $2b_0 c y_0 = \log^2(Q_0^2/\Lambda_{\text{QCD}}^2)$ . Insisting that (1) be valid at least in the  $y \rightarrow 0$  limit again provides us with a phenomenological value for the constant  $c$  in terms of the saturation momentum at  $y = 0$ . The form (2) leads to a notably slower growth of  $Q_s$  at high energy. Specifically, for central proton-nitrogen collisions at RHIC, LHC and GZK-cut-off energies (total rapidity  $y = 10.7, 17.3$  and  $26.0$ ) the saturation momentum of the nucleus in the rest frame of the projectile hadron is  $Q_s = 1.4, 4.5, 19.2$  GeV for fixed coupling evolution, while for running coupling evolution it is  $Q_s = 1.1, 2.4, 5.9$  GeV, respectively. Clearly, cosmic ray interactions in our atmosphere offer a realistic opportunity for observing this effect.

The dominant process for fast particle production ( $x_F \gtrsim 0.1$ ) is scattering of quarks from the incident dilute projectile on the dense target. At high energies (i.e. in the eikonal approximation where  $p^+$  is conserved), the transverse momentum distribution of quarks is given by the correlation function of two Wilson lines  $V$  running along the light cone at transverse separation  $r_t$  (in the amplitude and its complex conjugate),

$$\sigma^{qA} = \int \frac{d^2 q_t d q^+}{(2\pi)^2} \delta(q^+ - p^+) \left\langle \frac{1}{N_c} \text{tr} \left| \int d^2 z_t e^{i\vec{q}_t \cdot \vec{z}_t} [V(z_t) - 1] \right|^2 \right\rangle. \quad (3)$$

Here, the convention is that the incident hadron has positive rapidity, i.e. the large component of its light-cone momentum is  $P^+$ , and that of the incoming quark is  $p^+ = xP^+$  ( $q^+$  for the outgoing quark). The two-point function has to be evaluated in the background field of the target nucleus. A relatively simple closed expression can be obtained [14] in the McLerran-Venugopalan model of the small- $x$  gluon distribution of the dense target [7]. In that model, the small- $x$  gluons are described as a stochastic classical non-abelian Yang-Mills field which is averaged over with a Gaussian distribution. The  $qA$  cross section is then given by [14]

$$q^+ \frac{d\sigma^{qA \rightarrow qX}}{d q^+ d^2 q_t d^2 b} = \frac{q^+}{P^+} \delta\left(\frac{p^+ - q^+}{P^+}\right) C(q_t) \\ C(q_t) = \int \frac{d^2 r_t}{(2\pi)^2} e^{i\vec{q}_t \cdot \vec{r}_t} \left\{ \exp \left[ -2Q_s^2 \int_{\Lambda} \frac{d^2 l_t}{(2\pi)^2} \frac{1}{l_t^4} \left( 1 - \exp(i\vec{l}_t \cdot \vec{r}_t) \right) \right] - 2 \exp \left[ -Q_s^2 \int_{\Lambda} \frac{d^2 l_t}{(2\pi)^2} \frac{1}{l_t^4} \right] + 1 \right\}. \quad (4)$$

This expression is valid to leading order in  $\alpha_s$  (tree level), but to all orders in  $Q_s$  since it resums any number of scatterings of the quark in the strong field of the nucleus. The saturation momentum  $Q_s$ , as introduced in eq. (4), is related to  $\chi$ , the total color charge density squared (per unit area) from the nucleus integrated up to the rapidity  $y$  of the probe (i.e. the projectile quark), by  $Q_s^2 = 4\pi^2 \alpha_s^2 \chi (N_c^2 - 1)/N_c$ . In the low-density limit,  $\chi$  is related to the ordinary leading-twist gluon distribution function of the nucleus, see for example [15].

The integrals over  $p_t$  in eq. (4) are cut off in the infrared by some cutoff  $\Lambda$ , which we assume is of order  $\Lambda_{\text{QCD}}$ . At large transverse momentum, the first exponential in (4) can be expanded order by order to generate the usual power series in  $1/q_t^2$  [16, 17], with the leading term corresponding to the perturbative one-gluon  $t$ -channel exchange contribution to  $qg \rightarrow qg$  scattering. On the other hand, for  $Q_s \sim q_t \gg \Lambda$  one obtains in the leading logarithmic approximation [17]

$$C(q_t) \simeq \frac{1}{Q_s^2 \log Q_s/\Lambda} \exp\left(-\frac{\pi q_t^2}{Q_s^2 \log Q_s/\Lambda}\right). \quad (5)$$

This approximation reproduces the behavior of the full expression (4) about  $q_t \sim Q_s$ , and hence the transverse momentum integrated cross section reasonably well. It is useful when the cutoff  $\Lambda \ll Q_s$ , that is, when color neutrality is enforced on distance scales of order  $1/\Lambda \gg 1/Q_s$ . If, however, color neutrality in the target nucleus occurs over distances of order  $1/Q_s$  [18] then  $\Lambda \sim Q_s$  and one would have to go beyond the leading-logarithmic approximation; work along those lines is in progress.

Consider the probability of inelastic scattering (i.e. *with* color exchange) to small transverse momentum. This is given by expression (4,5), integrated from  $q_t = 0$  to  $q_t = \Lambda$ :

$$\int_0^{\Lambda} d^2 q_t C(q_t) \simeq \frac{\pi \Lambda^2}{Q_s^2 \log Q_s/\Lambda} + \dots \quad (6)$$

Here, we have written only the leading term in  $\Lambda^2/Q_s^2$ , neglecting subleading power-corrections and exponentially suppressed contributions. Hence, soft forward inelastic scattering is power-suppressed in the black-body limit. This steepens the longitudinal distribution  $dN/dx_F$  of leading particles since partons with large relative momenta fragment independently [5, 19].

We now turn to gluon bremsstrahlung which dominates particle production at  $x_F \lesssim 0.1$ . Gluon radiation with transverse momentum  $q_t \sim Q_s$  in high-energy hadron-nucleus collisions has been discussed in detail in [20, 21]; here we employ the latter *ansatz* for the fusion of gluon ladders:

$$E \frac{d\sigma}{d^3q} = 4\pi \frac{N_c}{N_c^2 - 1} \frac{1}{q_t^2} \int^{q_t^2} dk_t^2 \alpha_s(k_t^2) \phi_h(x_1, k_t^2) \phi_A(x_2, (q_t - k_t)^2), \quad (7)$$

where  $\phi(x, Q^2)$  denotes the unintegrated gluon distribution function of the projectile hadron or target nucleus, respectively. It is related to the gluon density by

$$x g(x, Q^2) = \int^{Q^2} dk_t^2 \phi(x, k_t^2). \quad (8)$$

The small- $x$  gluon density has been investigated recently within RG-improved QCD evolution equations by Ciafaloni et al. [11]. It predicts the onset of nonlinear (saturation) effects at transverse momenta similar to our values for  $Q_s(x)$ . Their gluon densities can be incorporated into phenomenological applications in the future.

For practical reasons, we presently employ the simpler Kharzeev-Levin *ansatz* for the infrared-finite gluon densities

$$x g(x, Q^2) \propto \frac{1}{\alpha_s} \min(Q^2, Q_s^2(x)) (1-x)^4, \quad (9)$$

with  $\alpha_s$  evaluated at  $\max(Q_s^2, Q^2)$ . In our approach, the absolute normalization is determined by energy conservation. The number of produced gluons behaves as  $dN/dq_t^2 \sim 1/q_t^4$  at large transverse momentum but flattens to  $\sim 1/q_t^2$  at  $q_t < \max(Q_s^A(x), Q_s^h(x))$  and finally approaches a constant in the  $q_t \rightarrow 0$  limit. Despite the rather qualitative nature of this *ansatz*, the main feature is that saturation effects provide an *intrinsic* semi-hard scale  $Q_s$  for partonic processes, thus eliminating the infrared divergences of leading-twist perturbation theory and, at the same time, the need for matching to some purely phenomenological models for low- $q_t$  particle production. In fact, the effects discussed here do not depend on details of our approach but follow generically from the fact that the *average* transverse momentum ( $\sim Q_s$ ) gets large as the BBL at high energy is approached.

For the application to cosmic-ray induced airshowers we have developed a Monte-Carlo algorithm which generates complete parton configurations as described above. The partons are then connected by strings. This accounts for the “absorption” of almost collinear gluons on the string, while independent fragmentation is reproduced when relative transverse momenta of partons are large. The fragmentation is performed via the Lund scheme as implemented in PYTHIA [22]. This model is linked to a standard pQCD event generator commonly used in air-shower computations (Sibyll v2.1 [23]) which handles low-energy and peripheral collisions where the saturation momentum of the nucleus is not sufficiently large. Finally, the hadron-nucleus collision models are embedded into the cascade equations which solve for the longitudinal profile of the airshower [24]. Details of our Monte-Carlo implementation will be published elsewhere.

Fluorescence detectors measure the number of charged particles (mostly  $e^\pm$ ) at a given atmospheric depth  $X$  which is given by the integral of the atmospheric density along the shower axis,  $X = \int ds \rho(s)$ . The position of the maximum defines  $X_{\max}$  which increases monotonically with the energy of the primary. Note that for nuclei the primary energy is shared by all of its nucleons and so  $X_{\max}$  also depends on the mass number: at fixed  $E$ , heavier primaries lead to smaller “penetration depth”  $X_{\max}$ .

In Figure 1 we compare the predictions of the leading-twist pQCD model Sibyll for proton and iron induced showers to the saturation model (BBL, for proton primaries only) with running and fixed coupling BFKL evolution of  $Q_s$ , respectively, and to preliminary Hires stereo data [1]. In the saturation limit, showers do not penetrate as deeply into the atmosphere. This is due to the “break-up” of the projectile’s coherence [19] together with the suppression of forward parton scattering (for central collisions). The comparison to the data suggests a light composition at those energies.

Also, contrary to present accelerator experiments, a clear difference between running-coupling and fixed-coupling BFKL evolution of the saturation momentum is apparent in this observable. The discrepancy between those evolution scenarios at the highest energies is strongly amplified by subsequent hadronic collisions in the cosmic ray cascade since it determines the fraction of events that occur close to the black-body limit (averaged over all impact parameters). Thus, assuming hadronic primaries, the extremely rapid growth of  $Q_s$  obtained for fixed coupling evolution is at

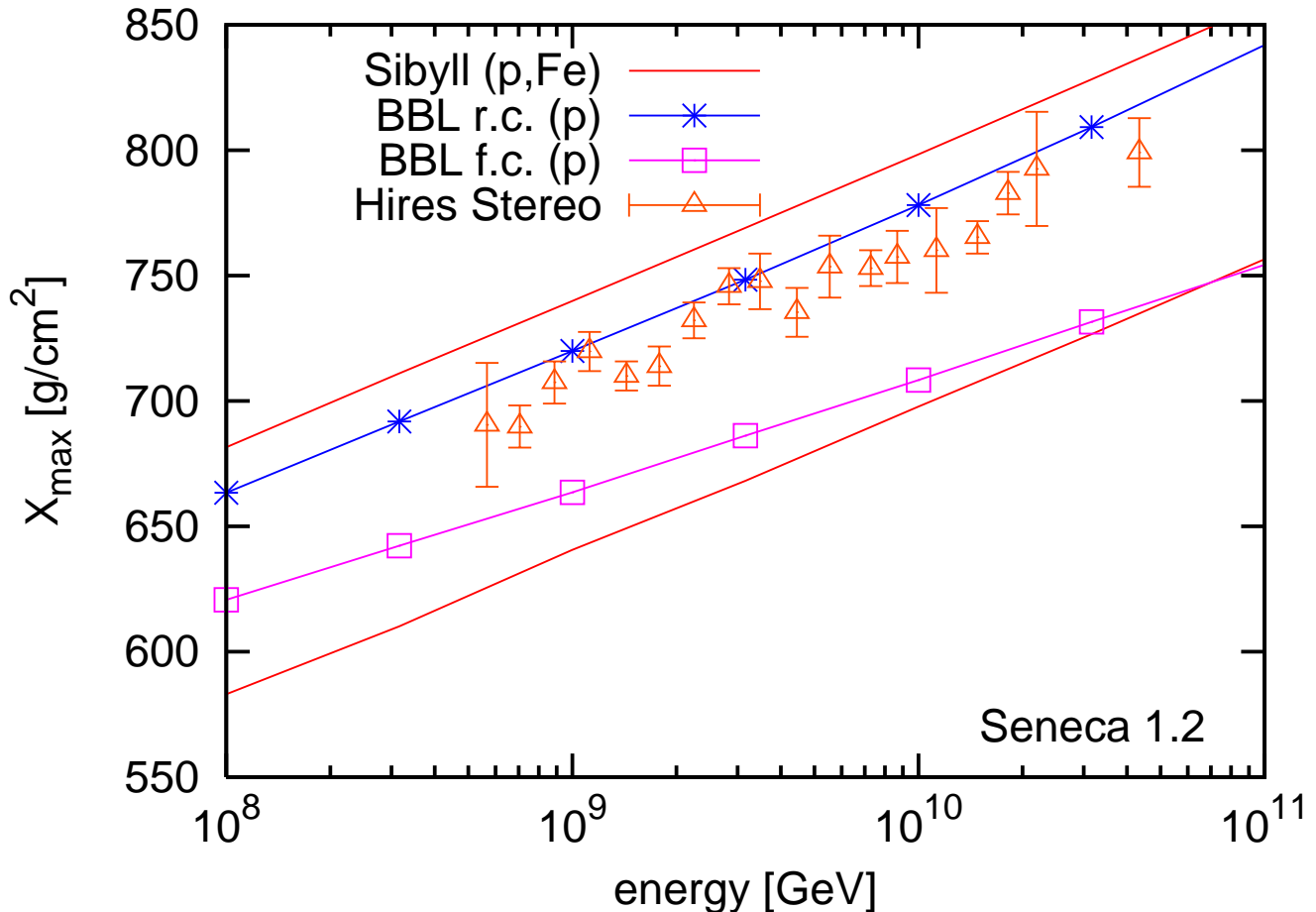


Figure 1:  $X_{\max}$  as a function of primary energy.

variance with the Hires data, as it would require hadrons lighter than protons. This is due to a too strong suppression of leading hadron production over a large range of impact parameters at high energies. At lower energies, of course, the two evolution scenarios predict similar saturation scales and so can not be distinguished as reliably by present collider experiments.

Finally, we remark that our results for running-coupling evolution coincide with those of another popular hadronic model, QGSJET [25]. Due to the absence of an ad-hoc  $q_t$  cutoff for pQCD interactions in QGSJET, that model needs to assume a rather flat gluon density  $\sim 1/\sqrt{x}$  at small  $x$  in order not to overestimate multiplicities at collider energies [4]. In our approach, on the other hand, the increase of the multiplicity and of the typical transverse momenta with energy is controlled by the saturation mechanism and the corresponding evolution of the gluon density.

In conclusion, we have shown that at energies near the GZK cutoff QCD evolution scenarios differ drastically in their predictions for the scale  $Q_s$  where gluon densities become nonperturbatively large (the BBL). Assuming hadronic primaries, properties of induced air showers suggest a moderately rapid growth of the gluon density with decreasing  $x$  (over a wide range of  $x$ ), corresponding to a more slowly increasing black-body scale  $Q_s$  with  $\log(1/x)$ . At least qualitatively, this agrees with a number of recent studies using extensions of DGLAP, resummations of  $\log x$  and  $\log Q$  effects, and running-coupling BFKL evolution [10, 11, 12, 13].

Fixed-coupling BFKL evolution, which is able to fit DIS at HERA [8] and deuteron-gold multiplicities at RHIC [21], predicts extremely large values for  $Q_s$  at GZK energies. From our analysis we conclude that its applicability is limited to much lower energies. We stress that measurements of hadron spectra in  $pA$  collisions at the LHC over a *broad* region of phase space (in particular, in the forward region) could majorly advance our knowledge of high-density QCD and, in turn, help us understand the nature, composition and perhaps the origin of the highest-energy cosmic rays.

## Acknowledgments

We thank R. Engel and L. Frankfurt for discussions. H.-J.D. acknowledges support by the German Minister for Education and Research (BMBF) under project DESY 05CT2RFA/7. The computations were performed at the Frankfurt Center for Scientific Computing (CSC).

- 
- [1] P. V. Sokolsky for the HiRes Collaboration, *Prepared for 28th International Cosmic Ray Conference (ICRC 03), Tsukuba, Japan, July 31 – Aug. 7, 2003*, p. 405; High Resolution Fly's Eye Collaboration, arXiv:astro-ph/0407622.
  - [2] S. Yoshida et al., *Astroparticle Physics* **3**, 105 (1995).
  - [3] J. Alvarez-Muniz, R. Engel, T. K. Gaisser, J. A. Ortiz and T. Stanev, *Phys. Rev. D* **66**, 033011 (2002); R. Engel, *Nucl. Phys. B (Proc. Suppl.)* **122**, 40 (2003); D. Heck, M. Risse and J. Knapp, *Nucl. Phys. Proc. Suppl.* **122**, 364 (2003).
  - [4] M. Zha, J. Knapp and S. Ostapchenko, preprint FZKA-6890ZE, *Prepared for 28th International Cosmic Ray Conferences (ICRC 2003), Tsukuba, Japan, 31 Jul - 7 Aug 2003*; S. S. Ostapchenko, *J. Phys. G* **29**, 831 (2003).
  - [5] L. Frankfurt, V. Guzey, M. McDermott and M. Strikman, *Phys. Rev. Lett.* **87**, 192301 (2001).
  - [6] A. H. Mueller, *Nucl. Phys. B* **558**, 285 (1999).
  - [7] L. McLerran and R. Venugopalan, *Phys. Rev. D* **49**, 2233 (1994); *ibid.* **49**, 3352 (1994); Y. V. Kovchegov, *ibid.* **54**, 5463 (1996); *ibid.* **55**, 5445 (1997);
  - [8] K. Golec-Biernat and M. Wusthoff, *Phys. Rev. D* **59**, 014017 (1999).
  - [9] E. Iancu and R. Venugopalan, arXiv:hep-ph/0303204, provides a detailed review of small- $x$  evolution and an extensive list of original references.
  - [10] D. N. Triantafyllopoulos, *Nucl. Phys. B* **648**, 293 (2003).
  - [11] M. Ciafaloni, D. Colferai, G. P. Salam and A. M. Stasto, *Phys. Rev. D* **68**, 114003 (2003).
  - [12] L. Frankfurt, M. Strikman and C. Weiss, arXiv:hep-ph/0311231.
  - [13] L. P. A. Haakman, O. V. Kancheli and J. H. Koch, *Nucl. Phys. B* **518**, 275 (1998); A. H. Mueller and D. N. Triantafyllopoulos, *Nucl. Phys. B* **640**, 331 (2002); see also K. Rummukainen and H. Weigert, arXiv:hep-ph/0309306.
  - [14] A. Dumitru and J. Jalilian-Marian, *Phys. Rev. Lett.* **89**, 022301 (2002).
  - [15] M. Gyulassy and L. D. McLerran, *Phys. Rev. C* **56**, 2219 (1997).
  - [16] F. Gelis and A. Peshier, *Nucl. Phys. A* **697**, 879 (2002); F. Gelis and J. Jalilian-Marian, *Phys. Rev. D* **67**, 074019 (2003).
  - [17] D. Boer and A. Dumitru, *Phys. Lett. B* **556**, 33 (2003); E. Iancu, K. Itakura and D. N. Triantafyllopoulos, arXiv:hep-ph/0403103.
  - [18] E. Iancu, K. Itakura and L. McLerran, *Nucl. Phys. A* **724**, 181 (2003).
  - [19] A. Dumitru, L. Gerland and M. Strikman, *Phys. Rev. Lett.* **90**, 092301 (2003) [Erratum-*ibid.* **91**, 259901 (2003)].
  - [20] Y. V. Kovchegov and A. H. Mueller, *Nucl. Phys. B* **529**, 451 (1998); B. Z. Kopeliovich, A. V. Tarasov and A. Schäfer, *Phys. Rev. C* **59**, 1609 (1999); A. Dumitru and L. D. McLerran, *Nucl. Phys. A* **700**, 492 (2002); A. Dumitru and J. Jalilian-Marian, *Phys. Lett. B* **547**, 15 (2002); J. P. Blaizot, F. Gelis and R. Venugopalan, arXiv:hep-ph/0402256.
  - [21] D. Kharzeev, E. Levin and L. McLerran, *Phys. Lett. B* **561**, 93 (2003); D. Kharzeev, E. Levin and M. Nardi, *Nucl. Phys. A* **730**, 448 (2004).
  - [22] T. Sjöstrand, et al., *Comp. Phys. Com.* **135**, 238 (2001).
  - [23] R. S. Fletcher, T. K. Gaisser, P. Lipari and T. Stanev, *Phys. Rev. D* **50**, 5710 (1994); R. Engel, T. K. Gaisser, T. Stanev and P. Lipari, *Prepared for 26th International Cosmic Ray Conference (ICRC 99), Salt Lake City, Utah, 17-25 Aug 1999*
  - [24] G. Bossard et al., *Phys. Rev. D* **63**, 054030 (2001); H. J. Drescher and G. Farrar, *Phys. Rev. D* **67**, 116001 (2003).
  - [25] N. N. Kalmykov, S. S. Ostapchenko and A. I. Pavlov, *Nucl. Phys. Proc. Suppl.* **52B**, 17 (1997).